Effect of Solvent on Surface Wettability of Electrospun Polyphosphazene Nanofibers

Yi-Jun Lin, Qing Cai, Qi-Fang Li, Li-Wei Xue, Ri-Guang Jin, Xiao-Ping Yang

Key Laboratory of Beijing City on Preparation and Processing of Novel Polymer Materials, Beijing University of Chemical Technology, Beijing 100029, China

Received 21 December 2008; accepted 19 March 2009
DOI 10.1002/app.30481
Published online 4 November 2009 in Wiley InterScience (www.interscience.wiley.com).

ABSTRACT: Two kinds of biodegradable polymers, poly(ε-caprolactone) (PCL) and poly[(alanino ethyl ester)$_{0.67}$ (glycino ethyl ester)$_{0.33}$ phosphazene] (PAGP), were electrospun by using four different solvents. All PCL nanofibrous mats had similar surface water contact angles independent of solvents. However, it was found that the water contact angles of PAGP nanofibrous mats were 102.2° ± 2.3°, 113.5° ± 2.2°, 115.8° ± 1.4°, and 119.1° ± 0.7°, respectively, when trifluoroethanol, chloroform, dichloromethane, and tetrahydrofuran were used as a solvent. This difference was supposed mainly due to phosphorous and nitrous atoms in PAGP being dragged to fiber surface with solvent evaporation during the solidification of nanofibers, because of the strong interaction between positive phosphorous atoms and electronegative atoms in solvents. This interaction was confirmed by Fourier Transform Infrared, and the accumulation of phosphorous and nitrous atoms in the solvent-casting PAGP film surface was identified by X-ray photoelectron spectrometry analysis. PCL samples did not show the solvent-controlled surface wettability because it contained fewer polar atoms. © 2009 Wiley Periodicals, Inc. J Appl Polym Sci 115: 3393–3400, 2010

Key words: electrospinning; nanofiber; polyphosphazene; surface wettability; biomaterials

INTRODUCTION

Electrospinning is a simple and an effective method for the production of ultrathin fibers,[1] which have diameters ranging from the nanometer to submicron scale.[2,3] In the past decade, this technique has been applied to prepare nanofibers of various biodegradable polymers, including synthetic and natural materials.[4–7] Because of the inherent high aspect ratio, specific surface area, and high porosity, electrospun nanofibers, which could mimic the natural extracellular matrix and enhance the cell migration and proliferation, are especially suitable for biomedical applications, for instance, scaffolds for tissue engineering and controlled drug delivery carriers.[8,9]

The diameter and surface morphology of electrospun fibers greatly depend on various parameters such as (i) solution parameters including concentration, viscosity, conductivity, and polarity, (ii) polymer characteristics including the average molecular weight of polymer and intermolecular reaction, and (iii) ambient parameters including temperature, humidity, and so forth.[10–13] All these are important factors in determining the wettability of nanofibrous mats. For example, fiber diameter and physical surface structure are known to drastically alter the surface wetting properties of the matrix. It is observed that with the decrease in fiber diameter and the increase in surface roughness of the electrospun fibers, wettablility of the matrix also decreases.[14]

At present, although various different types of polymers have been electrospun, many applications are still limited by a lack of materials that allow precise control of the surface characteristics. Besides the intrinsic chemical structure of the polymer, controlled hydrophobic or hydrophilic surface of scaffold plays an important role in tissue engineering, which affects cell behaviors, transfer of nutrition, and stabilization of the scaffold. It has been widely accepted that solvents with high dielectric value or good conductivity are excellent for electrospinning,[15,16] and it has been well understood that rougher fiber surface will form with faster volatile solvent used for electrospinning.[9,17] However, reports regarding the effect of solvent on surface chemical composition and wettability of electrospun nanofibers could be scarcely found. And it is hard to deduce a common conclusion on this aspect from different literatures, because many factors will influence the surface wettability of electrospun nanofibers even if they have used the same polymer.[18–20]

Correspondence to: Q. Cai (caiqing@mail.buct.edu.cn).
Contract grant sponsor: National Natural Science Foundation of China; contract grant number: 50873012.

On the contrary, polyorganophosphazenes offer opportunities for the tuning of surface properties that are not found for many conventional materials.[21] Changes in the side groups linked to the polyphosphazene skeleton allow the surface wetting character to be changed. Moreover, polyorganophosphazenes contain numerous polar atoms such as phosphorus, nitrogen, and oxygen and can have strong intermolecular reactions with polar solvents. It is believed that such interaction might cause differences in surface compositions during the solidification of electrospun nanofibers when different solvents are used. Therefore, polyorganophazenes could be proper polymers to investigate the effect of different solvents on the surface properties of electrospun nanofibers, but reports on electrospun biodegradable polyphosphazene nanofibers were limited.[22,23]

In this article, poly[(alanino ethyl ester)$_{0.67}$ (glycino ethyl ester)$_{0.33}$ phosphazene] (PAGP) and poly(ε-caprolactone) (PCL) were synthesized and electrospun by using trifluoroethanol (TFE), chloroform (TCM), dichloromethane (DCM), or tetrahydrofuran (THF) as a solvent. In comparison, PAGP and PCL solvent-casting films were also prepared from the four solvents. The wettability of the nanofibrous mats and the solvent-casting films was determined by static water contact angle (WCA). Surface compositions of solvent-casting films were determined by X-ray photoelectron spectrometry (XPS) measurement. The interaction between PAGP and solvent was identified by Fourier Transform Infrared (FT-IR). At last, a model was proposed to interpret the groups migration in PAGP samples with the evaporation of solvents.

EXPERIMENTAL

Materials

Hexachlorocyclotriphosphazene (purity of 99%, Bo Yuan New Material & Technique Co. Ltd., Ningbo, China) was purified by being recrystallized with anhydrous heptane and vacuum sublimed at 50°C (0.05 mmHg). ε-Caprolactone (Aldrich) was dried with CaH_2 and vacuum distilled (64°C/1.5 mmHg). All other reagents and solvents used were of analytical grade and supplied by Beijing Chemical Reagent Co., Ltd. (Beijing, China). Alanino ethyl ester hydrochloride and glycino ethyl ester hydrochloride were vacuum dried at 30°C for 12 hr. Triethylamine and benzene were refluxed with CaH_2 and sodium, respectively, and then distilled. TFE, THF, DCM, and TCM were directly used without further purification.

PCL (M_w = 50,000) was obtained by ring-opening polymerization of ε-caprolactone (Aldrich), which was synthesized at 130°C for 30 hr in the presence of 0.05 wt % $Sn(Oct)_2$ upon the addition of cetanol.

Synthesis of PAGP

PAGP was synthesized as described in the previous articles.[24–26] Briefly, polydichlorophosphazene ($PNCl_2$, 0.1 mol), which was prepared by thermal ring-opening polymerization of hexachlorocyclotriphosphazene, was dissolved in benzene (100 mL). Then, the solution was precooled to 0°C and a solution of amino acid ester was added slowly, which was prepared by refluxing alanino ethyl ester hydrochloride (0.6 mol) and triethylamine (0.6 mol) in benzene for 3 hr. The mixture was stirred continuously first at 0°C for 6 hr and then at room temperature for 48 hr. Subsequently, benzene solution of glycino ethyl ester (0.2 mol), prepared as earlier, was added dropwise to the mixture. The reaction was continued for another 24 hr at room temperature. After the insoluble hydrochloride salts were removed by filtration, the resulting polymeric solution was concentrated by vacuum evaporation of benzene and precipitated into petroleum ether (bp: 60–90°C) yielding a solid polymer. The polymer was vaccum-dried at 30°C for further use and the yield was 70% based on $(NPCl_2)_n$.

Preparation of electrospun fibrous mats

Transparent polymer solutions with concentration of 15% (w/v) were prepared by dissolving PAGP in TFE, TCM, DCM, or THF and stirred for 24 hr at room temperature. Then, the solutions were electrospun from a 10 mL vitreous syringe equipped with a blunt stainless steel nozzle (inner diameter = 0.91 mm), which was continuously pushed by a microinfusion pump (WZ-50CZ, Zhejiang University Medical Instrument Co., Ltd., Hangzhou, China) at a constant flow rate of 0.8 mL/hr. A high voltage (Beijing Institute of High Voltage Technology & Equipment, Beijing, China) was applied to the tip of the nozzle when a fluid jet was ejected. The distance between the nozzle tip and the collector, which was a flat aluminum plate, was 10 cm. In comparison, PCL (M_w = 50,000) nanofibrous mats were obtained in a similar way by using the same solvents.

Preparation of polymeric films by solvent casting

As a comparison, polymeric films were prepared by a solvent-casting method. Briefly, PAGP or PCL was dissolved at a concentration of 10% (w/v) in TFE, TCM, DCM, or THF and then the solutions were cast onto Telflon dishes. After solvent evaporation, the polymer-coated dishes were placed in a vacuum dryer overnight to remove any remaining solvent and polymeric films of approximately 80 to 120 μm thickness were obtained.

Characterization

Chemical structure

The synthesized PAGP was characterized via ^{1}H NMR analysis (AV600, Bruker, Germany, solvent of $CDCl_3$, ppm), and intrinsic viscosity was determined by using chloroform as a solvent at 30°C. The chemical analyses of PAGP in different solvents were performed by FT-IR spectroscopy (Nicolet 5700 with resolution of 4.0 cm^{-1}, Thermo Company, Madison, WI). The Nicolet spectrometer system with an Avatar Omni Sampler accessory and specimen was prepared in a horizontal sample cell.

Morphology and diameter of electrospun nanofibers

The morphology of electrospun nanofibers was observed with a field emission scanning electron microscope (SEM, S-4700, Hitachi, Japan) at an accelerating voltage of 20 kV. Before being imaged with SEM, samples were sputter coated with gold (JEOL JFC-1200 fine coater). Fiber diameters were measured from SEM micrographs by using image analysis software (Image J, National Institutes of Health, Bethesda, MD). Interfiber distance was calculated by measuring the distance between a fiber and the closest adjacent fiber within the same plane. A minimum of 80 fibers were calculated for each group.

Surface wettability and composition

Hydrophilicity of all the obtained nanofibrous mats and solvent-casting films was measured with a static contact angle instrument (JC2000C1, Shanghai Glory Numeral Technique & Device Co., Ltd., Shanghai, China), in which, 0.25 μL of deionized water was automatically dropped onto the sample and WCA was determined within 10 sec. Five samples were used for each test.

Surface compositions of solvent-casting films were determined by an XPS (Thermo V6 ESCALAB 250, Britain.), and the incidence angle of Al K_α ray was 90°.

Statistical analysis

All data presented were expressed as mean ± SD. Statistical analysis was carried out using single-factor ANOVA. A value of $P \leq 0.05$ was considered statistically significant.

RESULTS

Structural analysis of PAGP

By identifying the chemical shifts of alanino ethyl ester and glycino ethyl ester via ^{1}H NMR analysis, as shown in Figure 1, the molar ratio of the two side groups was calculated according to the integral areas of peak c and d (e). The PAGP used in electrospinning contained about 67 mol % alanino ethyl ester and 33 mol % glycino ethyl ester in its side groups. And the polymer had an intrinsic viscosity of 0.95 dL/g (30°C, $CHCl_3$).

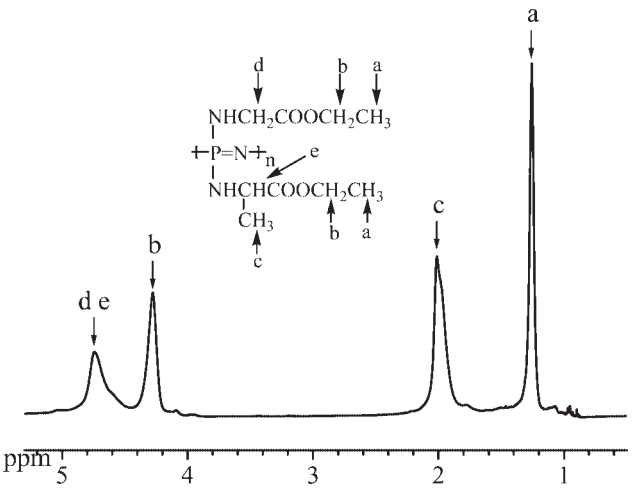

Figure 1 ^{1}H NMR spectrum of the produced PAGP.

Surface wettability of electrospun nanofibrous mats and solvent-casting films

The morphologies of electrospun PAGP and PCL mats produced with different solvents were observed with SEM, and the results were shown in Figures 2 and 3, respectively. Average fiber diameters and interfiber distances were calculated and listed in Table I. Obviously, all of them were composed of smooth and nanosized fibers with similar fiber surface morphologies. The average fiber diameters varied from 200 to 500 nm depending on the solvent being used. Moreover, all the electrospun mats exhibited similar interfiber distances that reveals their similar fiber depositions.

However, it was interesting to note that the electrospun PAGP mats prepared from different solvents showed different surface wettability. As shown in the insets in Figures 2 and 4, the PAGP nanofibrous mats were more and more hydrophobic in the order of TFE, TCM, DCM, and THF, and their WCAs were 102.2 ± 2.3°, 113.5° ± 2.2°, 115.8° ± 1.4°, and 119.1° ± 0.7°, respectively. However, this phenomenon did not occur in PCL nanofibrous mats, which exhibited about 123° whatever solvent was used. In comparison, WCAs of both solvent-casting PAGP and PCL films, which were prepared from the same solvents, were also measured and shown in Figure 4. In the case of PAGP films, they were 78.5° ± 1.2°, 80.3° ± 0.9°, 83.8° ± 1.5°, and 84.4° ± 1.6°, respectively, when TFE, TCM, DCM, or THF

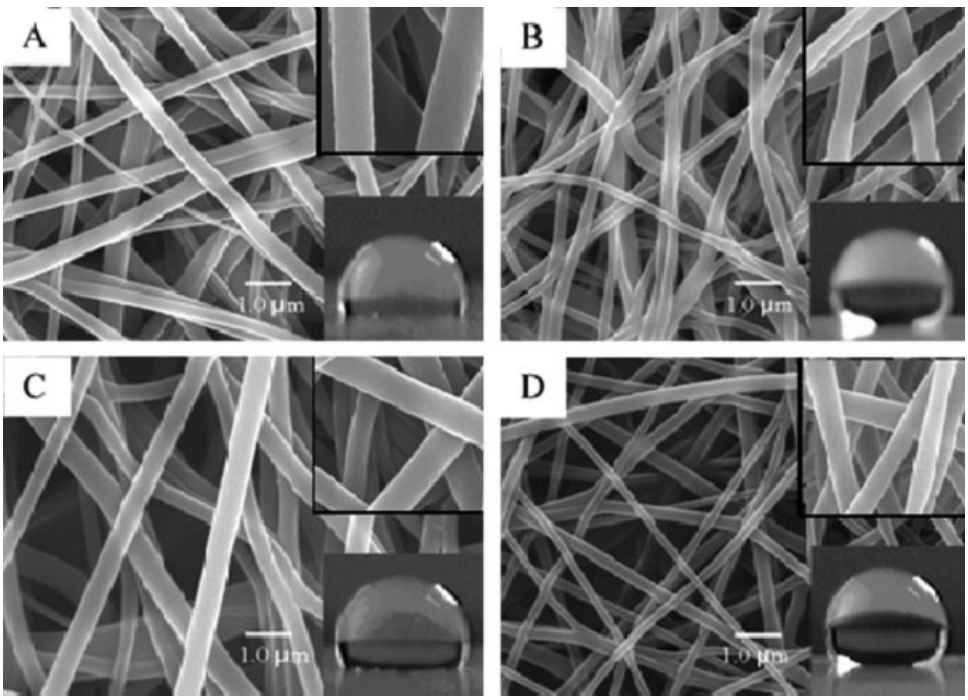

Figure 2 Morphology and hydrophilicity of electrospun PAGP nanofibrous mats prepared from different solvents: TFE (A), TCM (B), DCM (C), and THF (D).

were used as a solvent. The four PCL films prepared from the corresponding solvents exhibited minor differences in their WCAs. Additionally, the difference between the hydrophilicity of PAGP and PCL was more significant in the form of nanofibrous mats than in the form of solvent-casting films.

Surface compositions

XPS was applied in the analysis of surface compositions of all the solvent-casting PAGP and PCL films. Except the sample prepared from THF, the data in Figure 5 and Table II clearly showed that the P/C

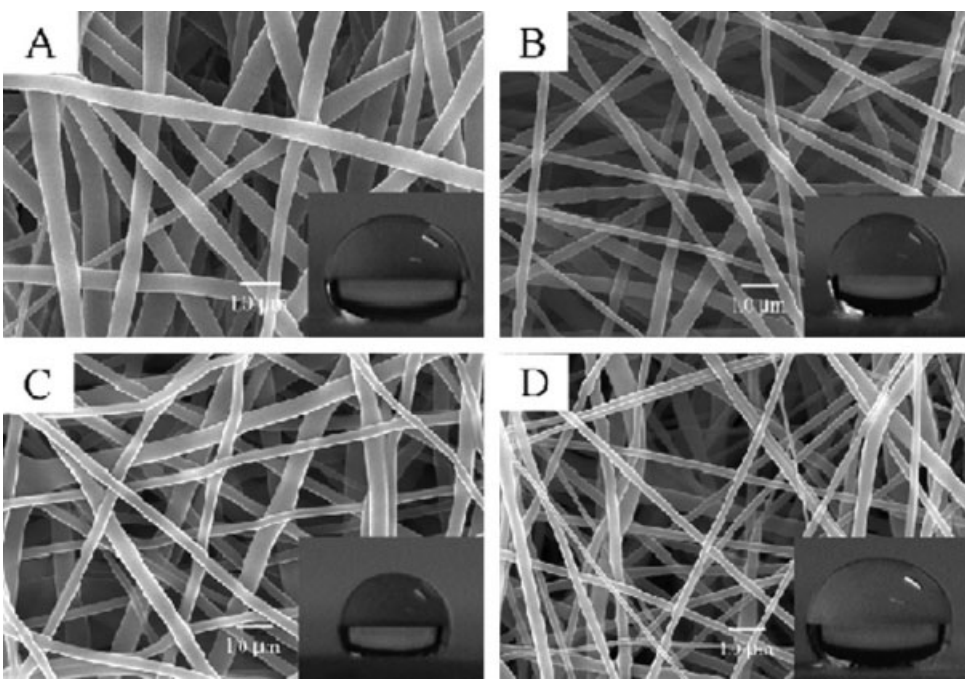

Figure 3 Morphology and hydrophilicity of electrospun PCL nanofibrous mats prepared from different solvents: TFE (A), TCM (B), DCM (C), and THF (D).

TABLE I
Average Fiber Diameter and Interfiber Distance of Electrospun PAGP and PCL Nanofibers by the Usage of Different Solvents

	Fiber diameter (nm)		Interfiber distance (nm)	
Solvent	PAGP	PCL	PAGP	PCL
TFE	433 ± 110	484 ± 83	1407 ± 243	1536 ± 312
TCM	381 ± 105	381 ± 52	1513 ± 253	1567 ± 371
DCM	506 ± 96	431 ± 74	1668 ± 235	1519 ± 296
THF	292 ± 117	226 ± 80	1574 ± 302	1492 ± 409

molar ratio was higher in the surface of PAGP films than those in the bulk for the other three solvents. On the contrary, the N/C and O/C molar ratios in the surface were lesser than those in the bulk. However, the contents of all of them increased steadily as the solvent being altered in the order of THF, DCM, TCM, and TFE. In the case of PCL films, the surface compositions varied slightly as different solvents were used. All the PCL samples demonstrated lower contents of O atoms in the surface than in the bulk.

Interaction between PAGP and solvents

The FTIR spectral analyses of PAGP dissolved in the four solvents were performed (Fig. 6). In the spectrum of solid PAGP sample, absorption peaks of —P=N— unit appeared at both 1220 cm^{-1} (symmetric stretching vibrations of —P=N— double bond) and 860 cm^{-1} (symmetric stretching vibrations of —P—N— single bond). However, the FTIR spectra of PAGP in the solution state showed that both the peaks shifted to the lower wavenumbers. The drift was larger as solvents being changed in the order of THF, DCM, TCM, and TFE. The absorption peak of carbonyl group around 1750 cm^{-1} also moved to lower wavenumbers slightly depending on the solvent.

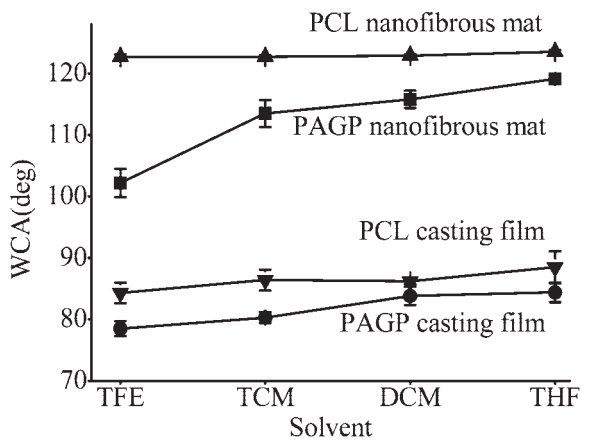

Figure 4 WCA data of electrospun PAGP and PCL nanofibrous mats and their corresponding solvent-casting films prepared from different solvents.

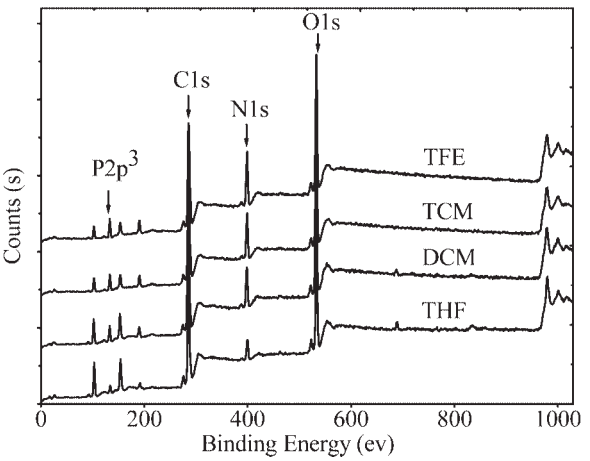

Figure 5 Overall XPS spectra of the four PAGP solvent-casting films prepared by using TFE, TCM, DCM, and THF as solvent.

DISCUSSION

Many studies have proven that a rough surface enhances the hydrophobicity by the presence of air on the surface, and the porous structure and interfiber distance contribute to the trapping of air.[27,28] An electrospun mat generally has a higher degree of surface roughness compared with its solvent-casting film[29] and results in a higher WCA. As shown in Figure 4, either electrospun PAGP or PCL mats were more hydrophobic than their corresponding solvent-casting films.

It was not surprising to find that both PCL nanofibrous mats and solvent-casting films had higher

TABLE II
Molar Ratios of Different Polar Atoms to Carbon Atom Calculated from XPS Data of PAGP and PCL Films

		Surface compositions			
Samples	Solvent	N/C	O/C	P/C	(N + O + P) /C
PAGP	TFE	0.248	0.386	0.168	0.802
	TCM	0.218	0.386	0.148	0.752
	DCM	0.184	0.368	0.128	0.680
	THF	0.094	0.363	0.065	0.522
	Theoretical*	0.320	0.427	0.107	0.854
PCL	TFE	–	0.303	–	–
	TCM	–	0.301	–	–
	DCM	–	0.296	–	–
	THF	–	0.293	–	–
	Theoretical*	–	0.333	–	–

"–" represents no data, the relative atom is absent.
The data were calculated from the stoichiometrical compositions of PAGP and PCL determined by ^1H NMR analysis.

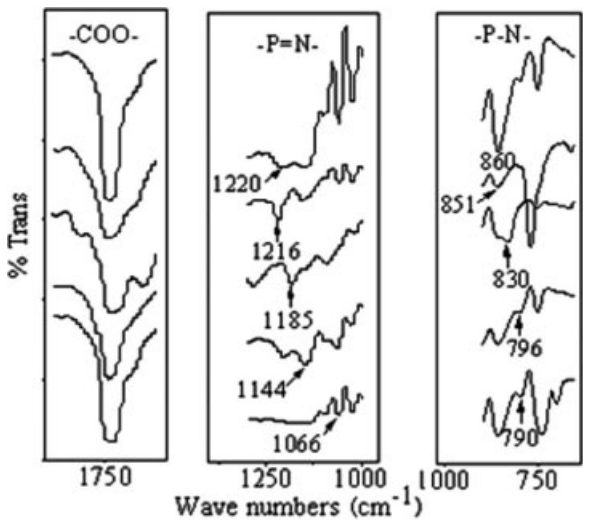

Figure 6 FT-IR spectra of PAGP in solution and solid states. From the top to down, the order was raw PAGP, the PAGP solution of THF, DCM, TCM, and TFE, respectively.

WCAs than relative PAGP samples, because PAGP contains more content of polar atoms. However, the surface WCA changed obviously in the case of PAGP, because different solvents being used to prepare the sample, whereas the WCA was almost constant in the case of PCL independent of solvent. Moreover, the difference in the hydrophilicity between PAGP and PCL turned to be more significant in nanofibrous mats than in solvent-casting films.

The fiber diameters of both PAGP and PCL nanofibrous mats varied with solvents (Table I), and some researchers proved that thinner fibers resulted in higher WCAs.[14,30,31] However, it was found that the four PCL nanofibrous mats had similar surface wettability in our study. This was thought due to their relatively minor difference in fiber diameters and interfiber distances; therefore, all the PCL nanofibrous mats should have similar roughness. The PAGP nanofibrous mats prepared from different solvents also contained fibers of similar diameters and interfiber distances, whereas it was confusing to understand why the surface of PAGP samples tended to be more hydrophobic in the order of TFE, TCM, DCM, and THF.

XPS data of PAGP films (Fig. 5) demonstrate that the surface contents of P, N, and O atoms vary with solvent. The increment in surface content was significant in the case of P and N atoms, when THF, DCM, TCM, and TFE was used to prepare the sample. In comparison with solid PAGP, FTIR analysis (Fig. 6) detected that the absorption peaks of —P=N— shifted when PAGP was dissolved in the four solvents, indicating that interaction had occurred between PGAP and the solvents. As is well known, phosphorus atoms in polyphosphazenes are liable to be attacked by nucleophilic agents for their cationic properties. On the other hand, F, Cl, and O atoms are all electronegative with the electronegativity values of 3.98, 3.16, and 3.44, respectively. Therefore, the four solvents used in this work could have strong interaction with PAGP via the static electronic interatomic reaction between electronegative atoms in the former and the cationic P atoms in the latter. Hydrogen bond might also be formed by means of imino groups of PAGP with TFE or THF. These interactions limited the vibration frequencies of —P=N— and =P—N= units, and caused the absorption peaks shifting to lower wavenumbers. The more the shift, the stronger is the interaction between the —P=N—P=N— backbone and the solvents, and here the order was TFE > TCM > DCM > THF. P and N atoms in PAGP films were suggested of being driven toward the film surface with solvent evaporation and led to the various surface wettability of PAGP films depending on the solvent. The interaction of carbonyl groups in the side groups of PAGP with solvents was weak, which was confirmed by two facts that (i) the shift of absorption peak of carbonyl groups was insignificant; and (ii) the content of oxygen atoms in sample surface changed little with solvent. And this was also one of the reasons to interpret the minor difference in surface contents of O atoms and WCAs of PCL films prepared from the four solvents.

Obviously, the migration of P and N atoms to fiber surface with solvent evaporation would also take place in preparing PAGP nanofibers by electrospinning to result in different surface chemical compositions. In the formation of solvent-casting films, the solvent evaporated at a relatively slow rate, which gave time to the rearrangement of different groups and did not cause too much difference in surface compositions. By the fact that all the nanofibers had smooth surfaces, the four solvents with different boiling points would evaporate at similar rates in the fast solidification of the electrospun nanofibers, which had not led to rough or porous fiber surface as reported.[32] With the fast solvent evaporation in electrospinning, the polar groups driven to fiber surface because of their interactions with solvents were immediately entrapped in the fiber surface. Thus, it would lead to more serious difference in surface compositions of electrospun PAGP nanofibers prepared from different solvents than those of corresponding films. This made the electrospun PAGP nanofibrous mats exhibit remarkably improved hydrophilicity by using THF, DCM, TCM, and TFE as solvents. When TFE was applied to electrospun PAGP, the WCA of the obtained nanofibrous mat could be reduced to $102.2^\circ \pm 2.3^\circ$, nearly 20° lesser than that as THF being used.

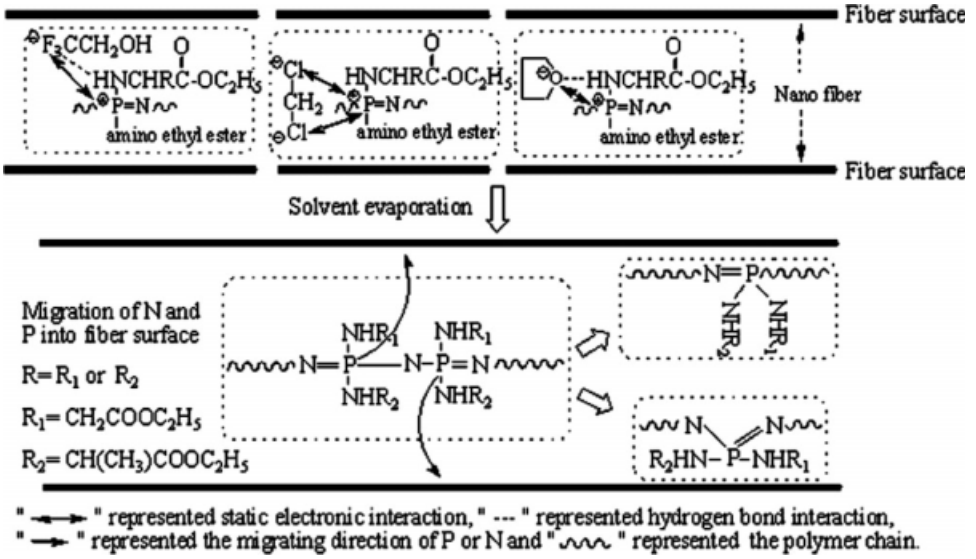

Figure 7 Schematic illustrations on the interaction of different solvents with PAGP and the migration of polar atoms to surface area.

According to these experimental results and discussion, a schematic illustration was proposed to describe the interaction between different solvents and PAGP, and the migration of P and N atoms to nanofiber/film surface region with solvent evaporation (see Fig. 7). Because of the strong polarity and small diameter of F atom, TFE could form strong hydrogen bonds with —NH— side groups of PAGP and existed static electronic interaction with PAGP between the electronegative F atoms and the cationic P atoms. These strong interactions drove the P and N atoms moving toward the fiber or film surface area during the solvent evaporation. THF could also interact with PAGP via the formation of hydrogen bonds with —NH— groups and the static electronic interaction with P atoms through its O atoms. But the interaction was weaker because O atom had lower electronegative value. And thus the contents of P and N atoms in the fiber or film surface area were remarkably increased when the solvent was changed from THF to TFE. When TCM and DCM were applied, although Cl atom showed the smallest electronegative value compared with F and O atoms, the migration of P and N atoms to sample surface was obvious. The surface contents of P and N atoms were even higher than those in the samples prepared from THF. These phenomena revealed that the effect of the static electronic interaction between solvents and PAGP on surface compositions depended strongly on the number of electronegative atoms in the solvent. The more the electronegative atoms in the solvent, the higher the content of P atoms in PAGP backbone dragged to the sample surface was. Nevertheless, those carbonyl groups in the side groups of PAGP had minor contribution to the different surface wettability of PAGP samples, because the molar ratios of O/C almost remained constant for all the solvent-casting PAGP films.

CONCLUSIONS

The properties of solvents could seriously affect the surface compositions and wettability of biodegradable amino acid ester substituted polyphosphazene film and electrospun nanofibers. The atomic electronegativity and the number of electronegative atoms in the solvent were the main reasons leading to the migration of P and N atoms thereof to the surface region of PAGP samples. This would provide an additional way to control the surface hydrophobicity/hydrophilicity of elecrospun fibrous scaffolds for tissue engineering.

References

1. Sarkar, S.; Deevi, S.; Tepper, G. Macromol Rapid Commun 2007, 28, 1034.
2. Greiner, A.; Wendorff, J. H. Angew Chem 2007, 46, 2.
3. Frenot, A.; Chronakis, I. S. Curr Opin Colloid Interface Sci 2003, 8, 64.
4. Huang, Z. M.; Zhang, Y. Z.; Kotaki, M.; Ramakrishna, S. Comp Sci Technol 2003, 63, 2223.
5. Young, Y.; Byung, M. M.; Seung, J. L.; Taek, S. L.; Won, H. P. J Appl Polym Sci 2005, 95, 193.
6. Li, M. Y.; Mark, J. M.; Milind, R. G.; Frank, K. K.; Anthony, S. W.; Peter, I. L. Biomaterials 2005, 26, 5999.
7. Geng, X. Y.; Kwon, O. H.; Jang, J. H. Biomaterials 2005, 26, 5427.
8. Smith, L. A.; Ma, P. X. Colloid Surf B 2004, 39, 125.
9. Travis, J. S.; Horst, A. V. Biomaterials 2008, 29, 1989.
10. Reneker, D. H.; Chun, I. Nanotechnology 1996, 7, 216.
11. Buchko, C. J.; Chen, L. C.; Shen, Y.; Martin, D. C. Polymer 1999, 40, 7397.

12. Deitzel, J. M.; Kleinmeyer, J.; Harris, D.; Beck Tan, N. C. Polymer 2001, 42, 261.
13. Tuteja, A.; Choi, W.; Ma, M. L.; Mabry, J. M.; Mazzella, S. A.; Rutledge, G. C.; Mckinley, G. H.; Cohen, R. E. Science 2007, 318, 1618.
14. Sangamesh, G. K.; Syam, P. N.; Roshan, J.; Lakshmi, S. N.; Cato, T. L. Biomaterials 2008, 29, 4100.
15. Lee, K. H.; Kim, H. Y.; Khil, M. S.; Ra, Y. M.; Lee, D. L. Polymer 2003, 44, 1287.
16. Li, N.; Qin, X. H.; Yang, E. L.; Wang, S. Y. Mater Lett 2008, 62, 1345.
17. Megelski, S.; Stephens, J. S.; Chase, D. B.; Rabolt, J. F. Macromolecules 2002, 35, 8456.
18. Fujihara, K.; Kotaki, M.; Ramakrishna, S. Biomaterials 2005, 26, 4139.
19. Kim, G.; Park, J.; Park, S. J Polym Sci Part B Polym Phys 2007, 45, 2038.
20. Mobarakeh, L. G.; Prabhakaran, M. P.; Morshed, M.; Hossein, M.; Esfahani, N.; Rama- Krishna, S. Biomaterials 2008, 29, 4532.
21. Allcock, H. R.; Steely, L. B.; Singh, A. Polym Int 2006, 55, 621.
22. Carampin, P.; Conconi, M. T.; Lora, S.; Menti, A. M.; Baiguera, S.; Bellini, S.; Grandi, C.; Parnigotto, P. P. Biomed Mater Res Part A 2006, 10, 661.
23. Nair, S. L.; Bhattacharyya, S.; Bender, J. D.; Greish, Y. E.; Brown, P. W.; Allcock, H. R.; Laurencin, C. T. Biomacromolecules 2004, 5, 2212.
24. Allcock, H. R.; Fuller, T. J.; Mack, D. P.; Matsumura, K.; Smeltz, K. M. Macromolecules 1977, 10, 824.
25. Allcock, H. R.; Cook, W. J.; Mack, D. P. Inorg Chem 1972, 11, 2584.
26. Zhang, T.; Hong, T.; Wu, Z. P.; Cui, F.; Cai, Q.; Jin, R. G. Polym Mater Sci Eng 2006, 22, 90.
27. Singh, A.; Steely, L.; Allcock, H. R. Langmuir 2005, 21, 11604.
28. Powell, H. M.; Boyce, S. T. J Biomed Mater Res A 2008, 84, 1078.
29. Demir, M. M.; Yilgor, I.; Erman, B. Polymer 2002, 43, 3303.
30. Robinette, E. J.; Palmese, G. R. Nucl Instrum Methods Phys Res B 2005, 236, 216.
31. Cui, W. G.; Li, X. H.; Zhou, S. B.; Weng, J. Polym Degrad Stab 2008, 93, 731.
32. Moroni, L.; Licht, R.; Boer, J.; Wijn, J. R.; Blitterswijk, C. A. Biomaterials 2006, 27, 4911.